NANO LETTERS

2007
Vol. 7, No. 11
3518−3522

Electric Field Effects on Spin Transport in Defective Metallic Carbon Nanotubes

Young-Woo Son,*,†,‡,§ Marvin L. Cohen,†,‡ and Steven G. Louie†,‡

Department of Physics, University of California at Berkeley, Berkeley, California 94720, Material Sciences Division, Lawrence Berkeley National Laboratory, Berkeley, California 94720, and Department of Physics, Konkuk University, Seoul 143-701, Korea

Received August 28, 2007

ABSTRACT

On the basis of first-principles calculations, we investigate transport properties of spin-polarized electrons in defective metallic single-wall carbon nanotubes (SWCNTs) under homogeneous transverse electric fields. Either vacancies or carbon adatoms are introduced in (10,10) SWCNT and are shown to play a role of quasi-localized magnetic impurities. The applied transverse electric fields change the relative position of the energy levels of the defects with respect to the Fermi energy so that the spin-polarized conductances are shown to be tunable. For some impurities, the orientation of the majority spin electrons in conducting channels at the Fermi energy can be switched to the opposite spin by an experimentally attainable electric field. Our results suggest that pure carbon or organic nanomagnets could be realized in SWCNTs, and their spin transport properties are controllable by transverse electric fields.

Single-wall carbon nanotubes (SWCNTs) have unique electrical transport properties that have attracted researchers from various disciplines since their discovery.[1,2] Among these, ballistic electron conduction has been studied theoretically for clean and defective SWCNTs,[3,4] and this property has been observed using various experimental configurations.[5] In addition to observing extremely long scattering lengths for the charge degree of freedom of electrons, spins in single- and multi-wall carbon nanotubes are also shown to propagate coherently over lengths as long as 0.2−1.5 μm.[6,7] This important property of spin-polarized electrons in SWCNTs has motivated their use in the emerging field of spintronics, which aims to control spins in electronic devices.[8]

To achieve spintronic devices based on SWCNTs, it is important to understand the role of impurities on transport properties of spin-polarized electrons. Although synthesis technology has advanced to make nearly defect-free SWCNTs,[9] very low densities of defects, for example, vacancies or carbon adatoms, are present.[10,11] Moreover, the localized orbitals of carbon atoms are magnetically active and are believed to be responsible for the observed magnetism in carbon-based nanostructures.[12,13] Because energy dependent spin-polarized carriers in typical spintronics devices (for example, spin valve systems) can change the magnetoresistance of the system qualitatively,[14,15] these localized orbitals at the impurity sites can change the spin-dependent conductance in SWCNTs when gate potentials or transverse electric fields are applied.[15,16]

Several recent experimental[12] and theoretical[13] studies have shown that the localized orbitals of undercoordinated carbon atoms at vacancies or those of carbon adatoms can give rise to net magnetic moments in carbon nanostructures. Magnetotransport in nanotubes in spin-valve systems[6,7,15−17] and chemically modified nanotubes[18,19] has been studied extensively; however, the influences of structural defects on the spin transport in SWCNTs has not. This property is important because the spin-dependent impurity states arising from a single defect[13] can block the conducting electrons near the Fermi energy (E_F) and can change the intrinsic spin transport properties because of the effect of gate voltages or electric fields.[20,21] In this study, we present a series of ab initio calculations of transport properties of spin-polarized electrons in (10,10) SWCNTs with either vacancies or carbon adatoms in the presence of an external transverse electric field (E_{ext}). The impurity states originated from the σ- and π-orbitals at vacancies produce multiple spin-dependent conductance dips around E_F. We show that the energy of these impurity states with respect to E_F can be varied as a function of the strength and direction of E_{ext} resulting in tunable spin conductance. Carbon adatoms either inside or outside the walls of nanotubes also play a role similar to that of magnetic impurities,[13] and their energies can be changed by E_{ext}. For a (10,10) SWCNT with a six-atom vacancy and one with a hydrogen-passivated carbon adatom inside, the orientation

* Corresponding author. E-mail: youngwoo@konkuk.ac.kr.
† University of California at Berkeley.
‡ Lawrence Berkeley National Laboratory.
§ Konkuk University.

10.1021/nl0721822 CCC: $37.00
Published on Web 10/31/2007

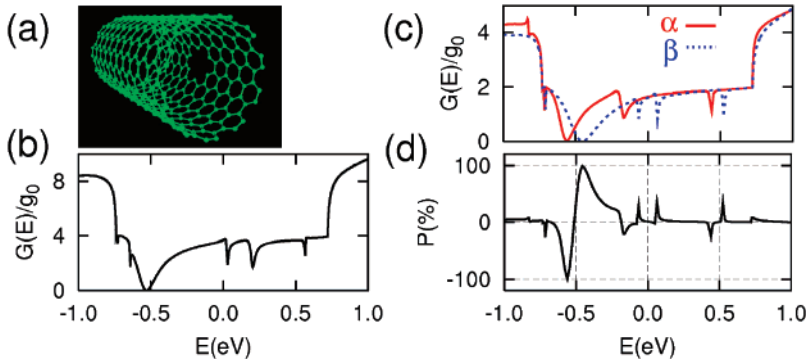

Figure 1. (a) Ball-and-stick model for (10,10) SWCNT with a 6DB defect. (b) Spin-unpolarized and (c) spin-polarized conductance of a defective (10,10) SWCNT shown in (a) without E_{ext}. In all figures, the solid red (dotted blue) lines denotes the conductance of α(β)-spin channel as a function of energy. The Fermi level (E_F) is set to zero in all figures. The conductance, $G(E)$, in all figures is plotted in a unit of $g_0 \equiv e^2/h$. (d) Spin polarization of conductance shown in (c), $P(\%) = 100\ (G_\alpha - G_\beta)/(G_\alpha + G_\beta)$ as a function of energy.

of the majority spin in conducting channels at E_F is shown to be reversed by experimentally achievable electric fields.

To study the spin-polarized conductance of defective nanotubes in electric fields, we employ first-principles calculations within the local spin density approximation (LSDA).[23] We introduce either carbon adatoms or vacancies into metallic nanotubes and describe their atomic and electronic structures using norm-conserving pseudopotentials with Kleinman−Bylander's nonlocal projectors.[24] To avoid interdefect interaction, 600 carbon atoms for the (10,10) nanotube in a supercell are considered and the wavefunction is expanded with a single-ζ basis set,[23] which was shown to be acceptable for nanotube-related systems.[25] The atomic structures with electric fields are fully relaxed until the forces on each of the atoms is less than 60 pN. A periodic saw-tooth type potential perpendicular to the direction of the tube axis is used to simulate the applied E_{ext} in a supercell. By calculating the spin-polarized scattering-state wavefunctions around the defects, we obtain the quantum mechanical probability for a spin-polarized electron near E_F to transmit through the defects.[21,22]

In two-probe measurements with ideal contacts to metallic leads, a (10,10) SWCNT has four conducting channels around E_F including the spin degeneracy. This system should have an electrical conductance of $15.5 \times 10^{-5}\ \Omega^{-1}$,[3,4] which is four times the unit of quantum conductance without spin degeneracy ($g_0 \equiv e^2/h = 3.9 \times 10^{-5}\ \Omega^{-1}$).[26] In clean (10,10) SWCNT with an applied electric field, the band dispersion at E_F is slightly modified near E_F, but the conductance does not change as there is no change in the number of conducting channels.[21,27] In contrast to the clean case, we expect large variations of spin conductances in defective nanotubes.

First, we study the spin-polarized conductance in a (10,10) SWCNT with a single large vacancy that is created by removing six carbons forming a hexagon (Figure 1a). This vacancy has six dangling bonds (DBs) and will be referred to as a 6DB hereafter. Without considering the spin degree of freedom, there are multiple narrow conductance dips around E_F originated from resonant scatterings by quasibound states from unsaturated σ-orbitals at the vacancy.[4] In addition to the narrow conductance dips, there is a broad conductance

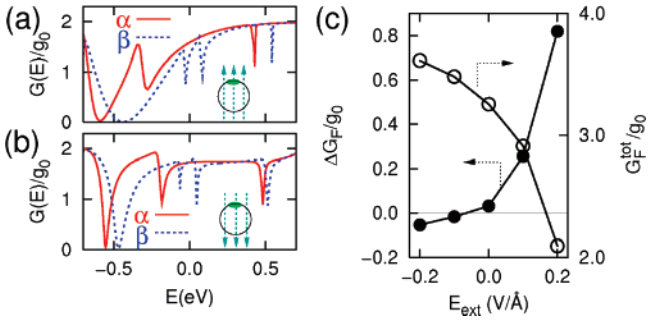

Figure 2. Spin-polarized conductance of (10,10) SWCNT with a 6DB when (a) $E_{ext} = +0.1$ and (b) -0.1 V/Å, respectively. Insets in (a) and (b) show the cross section of the nanotube (solid circle), vacancy (green elipse) and applied transverse electric fields (dotted arrows). The direction is positive when arrows point to the vacancy side. (c) The conductance difference at E_F, $\Delta G_F \equiv G_\alpha(E = E_F) - G_\beta(E = E_F)$ (left ordinate) and total conductance at E_F, $G^{tot}_F \equiv G_\alpha(E = E_F) + G_\beta(E = E_F)$ (right ordinate) of the (10,10) SWCNT shown in Figure 1a as a function of E_{ext} (abscissa).

dip at 0.53 eV below E_F where all incoming states are reflected due to a resonant scattering by impurity states from the π-orbitals of the edge atoms at the 6DB (Figure 1b).

Upon inclusion of the spin degree of freedom within the LSDA, all quasibound states are split into two spin channels and the conductance of each spin channel changes accordingly (Figure 1c). We will call one spin orientation an α-spin and the other a β-spin and shall defer the discussion of weak spin−orbit interactions to later. The total magnetic moment in this system is 3.04 μ_B where μ_B is the Bohr magneton. There is a broad conductance dip below E_F for each of the spin channels, showing complete backscattering for α- and β-spin electrons, respectively. Hence, there are perfect spin-polarized channels for the α- and β-spin at 0.45 and 0.56 eV below E_F, respectively, as shown by the spin polarization of the conductance (P) as a function of energy in Figure 1d. The conductance difference for α- and β-spin channels at E_F (ΔG_F shown in Figure 2c) is 0.03 g_0 only. With an applied electric field as discussed next, however, the magnitude of ΔG_F increase significantly.

In the presence of transverse electric fields, the screened electrostatic potential near the 6DB is altered so that the energy of the quasibound states originating from the 6DB

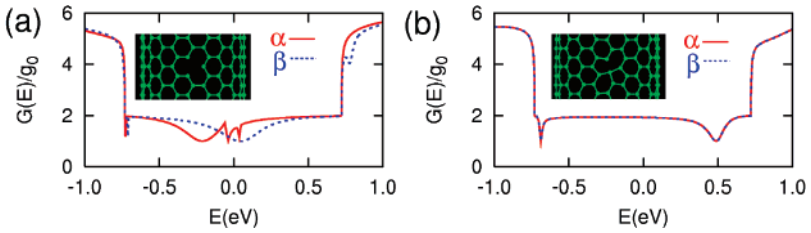

Figure 3. Calculated spin-polarized conductance of (10,10) SWCNT with (a) 3DB and (b) 5-1DB vacancy respectively. Insets display ball-and-stick models for each configuration.

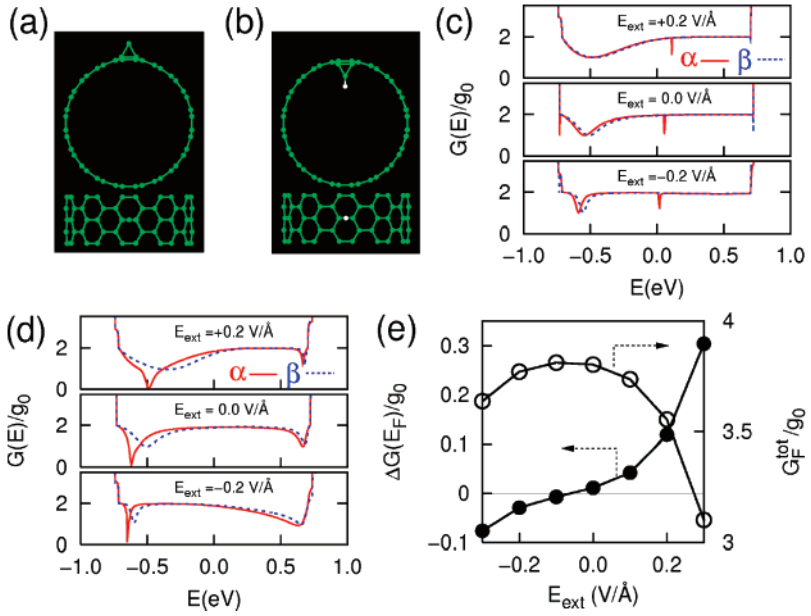

Figure 4. A ball-and-stick model for (a) a single carbon adatom outside (10,10) SWCNT and (b) a single carbon adatom passivated by a hydrogen inside (10,10) SWCNT. The upper (lower) figure in (a) and (b) show the cross sectional (top) view. From top to bottom panels in (c) and (d), the transmission spectra of the up (down)-spin channel of the defective (10,10) SWCNT shown in (a) and (b), respectively, where $E_{ext} = -0.2$, 0.0, and 0.2 V/Å, respectively. The direction of the electric field follows the same convention shown in Figure 2. (e) The conductance difference (ΔG_F) at E_F (left ordinate) and total conductance (G^{tot}_F) at E_F (right ordinate) of the (10,10) SWCNT with a carbon adatom passivated by a hydrogen (shown in b) as a function of E_{ext} (abscissa).

can be varied as a function of electric field.[21] The corresponding resonant backscattering, spin conductances at E_F, and the total magnetic moments are also anticipated to change in electric fields. When $E_{ext} > 0$ (electric field points toward the defect side, see inset in Figure 2a), the potential at the vacancy side is raised so that the corresponding energies for the quasibound states are increased irrespective of their spin orientation (Figure 2a). Similarly, with $E_{ext} < 0$, the energies of the quasibound states originated from the 6DB are decreased as the strength of the electric field is increased. The resulting variations of conductance for each spin orientation at E_F are summarized in Figure 2c. The total conductance at E_F is monotonically decreased when the electric field is changed from −0.2 to 0.2 V/Å. Notably, it is shown that the orientation of the majority spin in the conducting channels at E_F can be switched from α- to β-spin at $E_{ext} = -0.06$ V/Å when E_{ext} is swept from 0 to −0.2 V/Å. The magnetic moments of the system are also varied from 3.04 μ_B without electric field to $m = 3.28$ and 2.99 μ_B when the field is 0.1 and −0.1 V/Å, respectively.

DBs at vacancies can be saturated by hydrogen atoms (or by other foreign atoms).[13] These can also induce changes of atomic structure such as coalescence and reconstruction,[28,29] which will change the magnetic moments of the vacancy defects and alter the spin conductance significantly. We find that upon adsorption of six hydrogens to each DB at the 6DB, the magnetic moment of the 6DB disappears completely and no spin dependent conductance occurs (not shown here). Even without hydrogen adsorption, the reconstruction of vacancies results in a huge variation of spin conductance. For example, when a single carbon atom is removed, there are three DBs making a vacancy defect that is denoted as a 3DB (inset in Figure 3a). As shown in previous studies,[28] we find that a 3DB is a metastable vacancy defect that can be stabilized by reconstructions. The magnetic moment of 1.28 μ_B for an unconstructed 3DB disappears when it transforms to a vacancy having one pentagon and one dangling bond (5-1DB).[28] This is displayed in the inset of Figure 3b. The corresponding spin-dependent conductance is expected to be changed accordingly. In a (10,10) SWCNT with a 3DB, there are multiple spin-dependent conductance dips that originate from resonant scattering due to either quasi-localized defect states of unsaturated three σ-orbitals (narrow dips) or from π-orbitals (wide dips). When consider-

ing the reconstruction from a 3DB to a 5-1DB, the conductance of α-spin electrons is identical to that of β-spins, that is, no spin-polarized conductance occurs, as shown in Figure 3b.

Next, we find that a single carbon adatom either outside or inside a (10,10) SWCNT (shown in Figure 4a,b) also induces spin-dependent impurity states that can reflect incoming electrons depending on their spin orientations. As found in previous studies,[13] without an electric field a single carbon adatom outside the (10,10) SWCNT has a magnetic moment of 0.27 μ_B. The magnetic moment in the system decreases (increases) to 0.13 (0.43) μ_B with $E_{ext} = \pm 0.2$ V/Å. The conductance difference between the two spin channels is negligible at E_F as shown in the middle panel of Figure 4c. The applied electric field can move conductance dips, but there are no appreciable changes of spin conductance at E_F as shown in the upper and lower panels in Figure 4c. Moreover, upon inclusion of hydrogen to the adatom outside the wall of tube the magnetic moment becomes zero and no spin-dependent conductance occurs (not shown here). A hydrogen-passivated carbon atom inside a (10,10) SWCNT[30] drawn in Figure 4b, however, shows a finite magnetic moment of 1.48 μ_B without an electric field.

Just as in the 6DB case, electric fields can change the energy of the spin-polarized quasilocalized state due to a hydrogen-passivated carbon atom so that the spin-polarized conductance and the magnetic moment are both expected to be altered (Figure 4d). The magnetic moment is decreased to 1.10 (1.02) μ_B when the magnitude of electric field is increased to 0.2 V/Å regardless of its direction. The conductances for two spin channels at E_F are nearly same ($\Delta G_F = 0.01\ g_0$) as shown in the middle panel of Figure 4d. Depending on the direction of E_{ext}, either quasilocalized hole or electron states shown in Figure 4d moves to E_F so that ΔG_F increase up to 0.3 g_0 when $E_{ext} = +0.3$ V/Å. As shown in Figure 4e, the total conductance at E_F is decreased for both directions of the electric fields while the conductance difference between two spin channels at E_F is decreased or increased depending on the direction of the applied field. As in the 6DB case, we note that the orientation of majority spin in conducting channel at E_F is reversed from the α- to β-spin channel at $E_{ext} = -0.05$ V/Å when the field is swept from 0 to −0.2 V/Å.

A few remarks are in order. (1) As discussed before,[21] the strength of E_{ext} to achieve the changes of spin polarity is inversely proportional to the square of the diameter of the nanotube. For example, in the case of (20,20) SWCNTs with the hydrogen-passivated carbon adatom, the spin polarization reversal at E_F is expected with $E_{ext} \approx 0.013$ V/Å, which can be easily achieved in typical experimental configurations.[20,31] (2) Since E_{ext} is a transverse field to the moving electrons along the nanotube, the electrons will experience an induced spin−orbit interaction together with the small intrinsic one. The magnitude of both spin−orbit interactions is quite small for carbon systems (10^{-3}∼10^{-4} meV)[32,33] so that long spin lifetimes are expected as observed in recent experiments.[7,15] (3) The magnetic impurities on metallic nanotubes can give rise to a Kondo resonance at low temperature.[34] The Kondo temperature, however, strongly depends on the characteristics of a system, for example, size of magnetic impurity, coupling strength, and diameter of tubes, and there are many open questions regarding this problem.[35] We believe that the quasilocalized nature of the spin-polarized impurities considered here and the possible increase of the diameter of SWCNTs will suppress the Kondo temperature sufficiently.[35]

In summary, from a series of ab initio calculations, we find that spin-polarized conductances can occur when DBs at vacancies are exposed to vacuum and when carbon atoms are adsorbed on the walls of (10,10) SWCNTs. The spin orientation of the majority channel at E_F can be switched to the opposite one by an E_{ext} in (10,10) SWCNTs with the 6DB or for the hydrogen-passivated carbon adatom configuration.

Acknowledgment. This research was supported by NSF Grant DMR04-39768 and by the Director, Office of Science, Office of Basic Energy under Contract No. DE-AC02-05CH11231. Y.-W. Son acknowledges support by the KOSEF grant funded by the MOST No. R01-2007-000-10654-0. Computational resources have been provided by NSF at the NPACI and DOE at the NERSC.

References

(1) Iijima, S.; Ichihashi, T. *Nature* **1993**, *363*, 603−605.
(2) Bethune, D. S.; Klang, C. H.; de Vries, M. S.; Gorman, G.; Savoy, R.; Vazquez, J.; Beyers, R. *Nature* **1993**, *363*, 605−607.
(3) (a) Ando, T. *J. Phys. Soc. Jpn.* **2005**, *74*, 777−817. (b) Charlier, J.-C.; Blasé, X.; Roche, S. *Rev. Mod. Phys.* **2007**, *79*, 677−732 and references therein.
(4) Choi, H. J.; Ihm, J.; Louie, S. G.; Cohen, M. L. *Phys. Rev. Lett.* **2000**, *84*, 2917−2920.
(5) (a) Frank, S.; Poncharal, P.; Wang, Z. L.; de Heer, W. A. *Science* **1998**, *280*, 1744−1746. Bachtold, A.; Strunk, C.; Salvetat, J.-P.; Bonard, J.-M.; Forró, L.; Nussbaumer, T.; Schönenberger, C. *Nature* **1999**, *397*, 673−675. (c) Liang, W.; Bockrath, M.; Bozovic, D.; Hafner, J. H.; Tinkham, M.; Park, H. *Nature* **2001**, *411*, 665−669.
(6) (a) Tsukagoshi, K.; Alphenaar, B. W.; Ago, H. *Nature* **1999**, *401*, 572−574. (b) Kim, J.-R.; So, H. M.; Kim, J.-J.; Kim, J. *Phys. Rev. B* **2002**, *66*, 233401. (c) Man, M. T.; Wever, I. J. W.; Morpurgo, A. F. *Phys. Rev. B* **2006**, *73*, 241401(R).
(7) Hueso, L. E.; Pruneda, J. M.; Ferrari, V.; Burnell, G.; Valdés-Herrera, J. P.; Simons, B. D.; Littlewood, P. B.; Artacho, E.; Fert, A.; Mathur, N. D. *Nature* **2007**, *445*, 410−413.
(8) Žutić, I.; Fabian, J.; Sarma, S. D. *Rev. Mod. Phys.* **2004**, *76*, 323−410.
(9) Hata, K.; Futaba, D. N.; Mizuno, K.; Namai, T.; Yumura, M.; Iijima, S. *Science* **2004**, *306*, 1362−1364.
(10) Hashimoto, A.; Suenaga, K.; Gloter, A.; Urita, K.; Iijima, S. *Nature* **2004**, *430*, 870−873.
(11) Fan, Y.; Goldsmith, B. R.; Collins, P. G. *Nat. Mater.* **2005**, *4*, 906−911.
(12) (a) Esquinazi, P.; Spemann, D.; Höhne, R.; Setzer, A.; Han, K.-H.; Butz, T. *Phys. Rev. Lett.* **2003**, *91*, 227201. (b) Talapatra, S.; Ganesan, P. G.; Kim, T.; Vajtai, R.; Huang, M.; Shima, M.; Ramanath, G.; Srivastava, D.; Deevi, S. G.; Ajayan, P. M. *Phys. Rev. Lett.* **2005**, *95*, 097201. (c) Shibayama, Y.; Sato, H.; Enoki, T.; Endo, M. *Phys. Rev. Lett.* **2000**, *84*, 1744−1747.
(13) (a) Lehtinen, P. O.; Foster, A. S.; Ma, Y.; Krasheninnikov, A. V.; Nieminen, R. M. *Phys. Rev. Lett.* **2004**, *93*, 187202. (b) Lehtinen, P. O.; Foster, A. S.; Ayuela, A.; Vehviläinen, T. T.; Nieminen, R. M. *Phys. Rev. B* **2004**, *69*, 155422. (c) Ma, Y.; Lehtinen, P. O.; Foster, A. S.; Nieminen, R. M. *New J. Phys.* **2004**, *6*, 68.
(14) George, J. M.; Pereira, L. G.; Barthélémy, A.; Petroff, F.; Steren, L.; Duvail, J. L.; Fert, A.; Loloee, R.; Holody, P.; Schroeder, P. A. *Phys. Rev. Lett.* **1994**, *72*, 408−411.
(15) Sahoo, S.; Kontos, T.; Furer, J.; Hoffmann, G.; Gräber, M.; Cottet, A.; Schönenberger, C. *Nat. Phys.* **2005**, *1*, 99−102.

(16) Fedorov, G.; Lassagne, B.; Sagnes, M.; Raquet, B.; Broto, J.-M.; Triozon, F.; Roche, S.; Flahaut, E. *Phys. Rev. Lett.* **2005**, *94*, 066801.
(17) (a) Kokado, S.; Harigaya, K. *Phys. Rev. B* **2004**, *69*, 132402. (b) Jensen, A.; Hauptmann, J. R.; Nygard, J.; Lindelof, P. E. *Phys. Rev. B* **2005**, *72*, 035419.
(18) Latil, S.; Triozon, F.; Roche, S. *Phys. Rev. Lett.* **2005**, *95*, 126802.
(19) Avriller, R.; Latil, S.; Triozon, F.; Blase, X.; Roche, S. *Phys. Rev. B* **2006**, *74*, 121406(R).
(20) Park, J.-Y. *Appl. Phys. Lett.* **2007**, *90*, 023112.
(21) Son, Y.-W.; Ihm, J.; Cohen, M. L.; Steven, S. G.; Choi, H. J. *Phys. Rev. Lett.* **2005**, *95*, 216602.
(22) Choi, H. J.; Cohen, M. L.; Louie, S. G. *Phys. Rev. B* **2007**, *76*, 155420.
(23) Soler, J. M.; Artacho, E.; Gale, J. D.; García, A.; Junquera, J.; Ordejón, P.; Sánchez-Portal, D. *J. Phys. Condens. Matter* **2002**, *14*, 2745 and references therein.
(24) (a) Troullier, N.; Martins, J. L. *Phys. Rev. B* **1991**, *43*, 1993−2006. (b) Kleinman, L.; Bylander, D. M. *Phys. Rev. Lett.* **1982**, *48*, 1425−1428.
(25) Artacho, E.; Sánchez-Portal, D.; Ordejón, P.; García, A.; Soler, J. M. *Phys. Status Solidi B* **1999**, *215*, 809−817.
(26) (a) Landauer, R. *Philos. Mag.* **1970**, *21*, 863−867. (b) Fisher, D. S.; Lee, P. A. *Phys. Rev. B* **1981**, *23*, 6851(R)−6854(R).
(27) (a) O'Keeffe, J.; Wei, C.; Cho, K. *Appl. Phys. Lett.* **2002**, *80*, 676−678. (b) Li, Y.; Rotkin, S. V.; Ravaioli, U. *Nano Lett.* **2003**, *3*, 183−187.
(28) (a) Lu, A. J.; Pan, B. C. *Phys. Rev. Lett*. **2004**, *92*, 105504. Ajayan, P. M.; Ravikumar V.; Charlier, J.-C. *Phys. Rev. Lett.* **1998**, *81*, 1437−1440.
(29) Lee, G.-D.; Wang, C. Z.; Yoon, E.; Hwang, N.-M.; Kim, D.-Y.; Ho, K. M. *Phys. Rev. Lett*. **2005**, *95*, 205501.
(30) Krasheninnikov, A. V.; Nordlund, K.; Sirviö, M.; Salonen, E.; Keinonen, J. *Phys. Rev. B* **2001**, *63*, 245405.
(31) Ishigami, M.; Sau, J. D.; Aloni, S.; Cohen, M. L.; Zettl, A. *Phys. Rev. Lett.* **2005**, *94*, 056804.
(32) De Martino, A.; Egger, R. *J. Phys.: Condens. Matter* **2005**, *17*, 5523−5532.
(33) Son, Y.-W.; Cohen, M. L.; Louie, S. G. *Nature* **2006**, *444*, 347−349.
(34) Odom, T. W.; Huang, J.-L.; Cheung, C. L.; Lieber, C. M. *Science* **2000**, *290*, 1549−1522.
(35) (a) Fiete, G. A.; Zarand, G.; Halperin, B. I.; Oreg, Y. *Phys. Rev. B* **2002**, *66*, 024431. (b) Wei, F.; Zhu, J.-L.; Chen, H.-M. *Phys. Rev. B* **2003**, *67*, 125410.

NL0721822